SETAC PRESS

Environmental Toxicology and Chemistry, Vol. 16, No. 11, pp. 2296–2303, 1997

Printed in the USA
0730-7268/97 $6.00 + .00

# MECHANISTIC QUANTITATIVE STRUCTURE–ACTIVITY RELATIONSHIP MODEL FOR THE PHOTOINDUCED TOXICITY OF POLYCYCLIC AROMATIC HYDROCARBONS: II. AN EMPIRICAL MODEL FOR THE TOXICITY OF 16 POLYCYCLIC AROMATIC HYDROCARBONS TO THE DUCKWEED *LEMNA GIBBA* L. G-3

XIAO-DONG HUANG, SERGEY N. KRYLOV, LISHA REN, BRENDAN J. MCCONKEY, D. GEORGE DIXON and BRUCE M. GREENBERG*
Department of Biology, University of Waterloo, Waterloo, Ontario N2L 3G1, Canada

(*Received* 5 *October* 1996; *Accepted* 28 *March* 1997)

**Abstract**—Photoinduced toxicity of polycyclic aromatic hydrocarbons (PAHs) occurs via photosensitization reactions (e.g., generation of singlet-state oxygen) and by photomodification (photooxidation and/or photolysis) of the chemicals to more toxic species. The quantitative structure–activity relationship (QSAR) described in the companion paper predicted, in theory, that photosensitization and photomodification additively contribute to toxicity. To substantiate this QSAR modeling exercise it was necessary to show that toxicity can be described by empirically derived parameters. The toxicity of 16 PAHs to the duckweed *Lemna gibba* was measured as inhibition of leaf production in simulated solar radiation (a light source with a spectrum similar to that of sunlight). A predictive model for toxicity was generated based on the theoretical model developed in the companion paper. The photophysical descriptors required of each PAH for modeling were efficiency of photon absorbance, relative uptake, quantum yield for triplet-state formation, and the rate of photomodification. The photomodification rates of the PAHs showed a moderate correlation to toxicity, whereas a derived photosensitization factor (PSF; based on absorbance, triplet-state quantum yield, and uptake) for each PAH showed only a weak, complex correlation to toxicity. However, summing the rate of photomodification and the PSF resulted in a strong correlation to toxicity that had predictive value. When the PSF and a derived photomodification factor (PMF; based on the photomodification rate and toxicity of the photomodified PAHs) were summed, an excellent explanatory model of toxicity was produced, substantiating the additive contributions of the two factors.

**Keywords**—Polycyclic aromatic hydrocarbons Phytotoxicology Photoinduced toxicity Photomodification Photosensitization

## INTRODUCTION

For ecotoxicologic modeling, quantitative structure–activity relationships (QSARs) are useful for correlating the physical properties of chemicals to given biological responses [1,2]. Such QSARs allow prediction of the potential hazards of untested compounds, identification of the physical traits of chemicals that contribute to their biological impacts, descriptions of the routes of chemical interaction with an organism, and elucidation of the mechanisms of toxicity. In developing a model, consideration of the attributes of the environmental compartment in which the contaminant of interest resides is essential, as this will dictate which of the contaminant's physical properties are likely to be most influential in toxicity. Because solar radiation is ubiquitous in the environment and can enhance the toxicity of polycyclic aromatic hydrocarbons (PAHs) [3–6], it represents a modifying environmental factor that should be considered in QSAR toxicity modeling for these chemicals.

The primary photochemical reactions of PAHs can impact negatively on living organisms [3–7]. In the companion paper [8], these principles were used to derive a theoretical QSAR model for photoinduced toxicity of PAHs based on photosensitization and photomodification reactions. Photosensitization reactions usually proceed via formation of highly reactive singlet-state oxygen ($^1O_2$) [5,7]. The process begins with the sensitizing molecule absorbing a photon, which elevates it to the excited singlet state [8,9]. From there the molecule can be transformed by intersystem crossing to the excited triplet state, where it can react with ground triplet-state oxygen ($^3O_2$) to form $^1O_2$. Singlet-state oxygen formed within a biological organism is highly damaging [10,11]. Photomodification of PAHs, which usually occurs via oxidation reactions [12,13], generally increases the toxicity of the PAHs by formation of new compounds with toxicologic properties distinct from the parent PAHs [6,13–15].

In the companion paper [8] distinct photosensitization constants (PSC) and photomodification constants (PMC) were derived for each PAH, to describe the contributions to toxicity of the photosensitization reactions and the impact of the photomodified compounds. Further, the PSC and PMC were theoretically shown to additively contribute to toxicity. This paper reports on the validation of the theoretical model based on independently measured parameters for each PAH that were suggested in the companion paper [8] to be determinants in photoinduced toxicity. *Lemna gibba L.* was chosen for this study and that in the companion paper [8] because at the level of photosynthesis and leaf morphology it is a typical C-3 plant [16]. However, because the leaves are in direct contact with the aqueous medium and the plant takes up chemicals through the underside of the leaf [16], QSAR modeling can be based on a two-compartment system, growth medium and leaf tissue. The parameters were the integral of the overlap between the

* To whom correspondence may be addressed.

Table 1. Physical constants and toxicity data used for the calculation of photosensitization factors (PSFs) and photomodification factors (PMFs). Toxicity is inhibition of growth of *Lemna gibba* by the intact polycyclic aromatic hydrocarbons (PAHs) ± standard deviation, $n = 9$. $[C_L]$, in μmol/g fresh weight, is plant uptake of PAH. φ is the quantum yield for triplet-state formation [20–23]. $J$ represents absorption of simulated solar radiation (SSR) by the PAH [8]. The PSF is the product of $[C_L]^n$, $\varphi^n$, and $J^n$ (the superscript n denotes that the respective values were normalized). $t_{1/2}$ is the half-life in h of the PAH in SSR, and $k_m$ ($h^{-1}$) is the exponential decay rate constant based on $t_{1/2}$ [8]. $T^n_{pm}$ is the normalized value of the toxicity (inhibition of growth) of the fully photomodified PAHs to *L. gibba*. The PMF is the product of $k^n_m$ and $T^n_{pm}$

| PAH[a] | Toxicity | $[C_L]$ | φ | $J$ | $[C_L]^n$ | $\varphi^n$ | $J^n$ | PSF | $t_{1/2}$ | $k_m$ | $k^n_m$ | $T^n_{pm}$ | PMF |
|---|---|---|---|---|---|---|---|---|---|---|---|---|---|
| ANT | 1.000 ± 0.024 | 0.080 | 0.60 | 36.9 | 0.250 | 0.63 | 0.119 | 0.019 | 2 | 0.347 | 1.000 | 1.00 | 1.000 |
| BAA | 0.745 ± 0.014 | 0.012 | 0.80 | 58.7 | 0.038 | 0.84 | 0.190 | 0.006 | 5 | 0.139 | 0.401 | 1.00 | 0.401 |
| BBA | 0.259 ± 0.038 | 0.035 | 0.65 | 37.0 | 0.109 | 0.68 | 0.120 | 0.009 | 27 | 0.026 | 0.075 | 0.97 | 0.073 |
| BBF | 0.354 ± 0.061 | 0.093 | 0.50 | 46.5 | 0.291 | 0.53 | 0.150 | 0.023 | 70 | 0.010 | 0.029 | 0.66 | 0.019 |
| BGP | 0.139 ± 0.043 | 0.054 | 0.60 | 126.2 | 0.169 | 0.63 | 0.408 | 0.044 | 100 | 0.007 | 0.020 | 0.26 | 0.005 |
| BAP | 0.255 ± 0.024 | 0.046 | 0.40 | 200.3 | 0.144 | 0.42 | 0.647 | 0.039 | 52 | 0.013 | 0.038 | 0.98 | 0.037 |
| BEP | 0.165 ± 0.057 | 0.051 | 0.70 | 78.8 | 0.159 | 0.74 | 0.255 | 0.030 | 75 | 0.009 | 0.026 | 0.78 | 0.020 |
| CHR | 0.016 ± 0.026 | 0.039 | 0.67 | 34.8 | 0.122 | 0.70 | 0.112 | 0.010 | 56 | 0.012 | 0.035 | 0.74 | 0.026 |
| COR | 0.118 ± 0.052 | 0.037 | 0.80 | 102.0 | 0.116 | 0.84 | 0.330 | 0.032 | 100 | 0.007 | 0.020 | 0.55 | 0.011 |
| DAA | 0.085 ± 0.038 | 0.058 | 0.50 | 144.2 | 0.181 | 0.53 | 0.466 | 0.044 | 16 | 0.043 | 0.124 | 0.17 | 0.021 |
| DAP | 0.458 ± 0.028 | 0.045 | 0.50 | 309.5 | 0.141 | 0.53 | 1.000 | 0.074 | 40 | 0.017 | 0.049 | 0.64 | 0.031 |
| FLA | 0.580 ± 0.061 | 0.288 | 0.60 | 84.8 | 0.900 | 0.63 | 0.274 | 0.156 | 40 | 0.017 | 0.049 | 0.88 | 0.043 |
| FLE | 0.160 ± 0.071 | 0.236 | 0.31 | 3.0 | 0.738 | 0.33 | 0.010 | 0.002 | 19 | 0.037 | 0.107 | 0.30 | 0.032 |
| PHE | 0.104 ± 0.043 | 0.320 | 0.80 | 8.9 | 1.000 | 0.84 | 0.029 | 0.024 | 14 | 0.050 | 0.144 | 0.27 | 0.039 |
| PYR | 0.170 ± 0.024 | 0.251 | 0.27 | 72.7 | 0.784 | 0.28 | 0.235 | 0.052 | 46 | 0.015 | 0.043 | 0.45 | 0.020 |
| TRI | 0.071 ± 0.043 | 0.094 | 0.95 | 8.9 | 0.294 | 1.00 | 0.029 | 0.008 | 65 | 0.011 | 0.032 | 0.58 | 0.018 |

[a] Names of PAHs are given in Figure 1.

spectrum of the simulated solar radiation (SSR) source and the absorption spectrum of the PAH ($J$), uptake of a given PAH ($[C_L]$), quantum yield for triplet-state formation (φ), rate of photomodification ($k_m$), and toxicity of a given photomodified PAH ($T_{pm}$). The parameters were combined to provide both predictive and explanatory QSAR models of toxicity.

## MATERIALS AND METHODS

Prior to chemical treatment, *L. gibba* L. G-3 was cultured axenically on half-strength Hutner's medium under 60 μmol $m^2$ s of continuous cool-white fluorescent light [6]. The irradiation source for plant growth during chemical treatment was SSR at a total photon fluence rate of 100 μmol $m^2$ s based on integration from 290 to 700 nm [6,8,15]. Plants were placed on 10 ml of fresh half-strength Hutner's medium in 5-cm petri dishes and exposed to a given PAH at 2 mg L for both the intact and photomodified forms as previously described [6,8]. In this set of experiments the PAHs and medium were not replenished during the experiment to allow sufficient time for the slowly photomodified PAHs to form large amounts of photoproducts.

The primary toxicity endpoint employed was inhibition of plant growth as determined by leaf production [16]. Plant growth was monitored over an 8-d period by counting leaves in 2-d intervals. Data for the number of leaves produced as a function of time were converted to growth rates of the plants and presented as inhibition of growth in the presence of a PAH. Toxicity was also assessed by measuring the fresh weight of the plants and quantifying the chlorophyll content of the leaves [16]. All toxicity tests were performed in triplicate with a minimum of three independent replicates per test ($n = 9$).

The data for the rate of PAH photomodification were taken from the companion paper [8] and are presented here in Table 1. Uptake of intact PAHs, $[C_L]$, was estimated by measuring the PAH concentration in the growth medium after incubation of *L. gibba* in medium containing 2 mg L of the intact PAH in darkness for 48 h. This period is sufficient for the chemicals to come to a steady state in plant tissue [17]. The dimethylsulfoxide (DMSO) delivery solvent does not change the kinetics of uptake [17]. Additionally, the chemicals were shown to occur in cellular membranes, not in leaf cuticles [17]. After incubation, the PAHs remaining in solution and adsorbed to the petri dish were assayed spectrophotometrically following dichloromethane extraction. The difference between the starting and the final concentrations was the amount taken up by the plant leaf, as the PAHs used are not lost by volatilization [18]. The amount of PAH taken up, $[C_L]$, was then calculated on a plant fresh weight basis (μmol/g fresh weight; Table 1). The data were then normalized to the PAH with the highest tissue concentration (phenanthrene) to generate relative tissue concentrations, $[C_L]^n$ (Table 1). Although this does not provide a bioaccumulation factor, it does allow ranking of the relative (or normalized) uptake of each PAH by *L. gibba,* which was sufficient for modeling. The tissue concentrations reported in Table 1 were consistent with the results of a recently completed extensive study on PAH uptake by *L. gibba* [17].

Linear and log-linear least squares regressions were performed to determine the quality of the correlation of a given parameter(s) to toxic strength. The regression analyses were performed with Sigma Plot (Jandel Scientific Software, San Rafael, CA, USA) and SYSTAT (*Version 5.05 for Windows,* Evanston, IL, USA). The strength ($r^2$) and significance ($p$) of the correlations are reported for each regression. Multiple regression analysis was also performed using SYSTAT. Standard deviations and standard errors were calculated as needed using SYSTAT (in all cases $n = 9$).

## RESULTS

### *Inhibition of plant growth in the presence of intact and photomodified PAHs in SSR*

When the intact PAHs were applied to the plants in the presence of SSR, inhibition of growth ranged from ≤10% (CHR, FLE, COR, and DAA [names of PAHS are given in Fig. 1]) to 97% (ANT) (Fig. 1 and Table 1). Growth inhibition for each of the 16 PAHs in photomodified form was also measured (Fig. 1) and ranged from about 20% for DAA to 100%

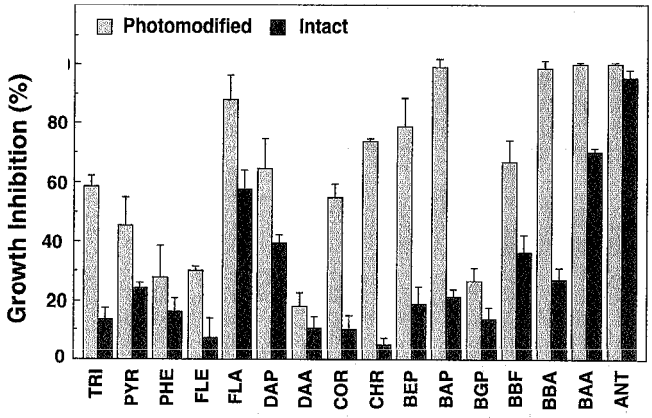


Fig. 1. Photoinduced toxicity of intact and photomodified polycyclic aromatic hydrocarbons (PAHs) to *Lemna gibba*. Plants were grown in simulated solar radiation with the chemicals at 2 mg/L. Growth was monitored by counting leaves and is presented as percent inhibition of growth relative to the controls. Error bars represent standard error of the mean ($n$ = 9). PAH abbreviations: anthracene, ANT; benzo[*a*]anthracene, BAA; benzo[*b*]anthracene, BBA; benzo[*b*]fluorene, BBF; benzo[*g,h,i*]perylene, BGP; benzo[*a*]pyrene, BAP; benzo[*e*]pyrene, BEP; chrysene, CHR; coronene, COR; dibenzo[*a,i*]anthracene, DAA; dibenzo[*a,h*]pyrene, DAP; fluoranthene, FLA; fluorene, FLE; phenanthrene, PHE; pyrene, PYR; triphenylene, TRI.

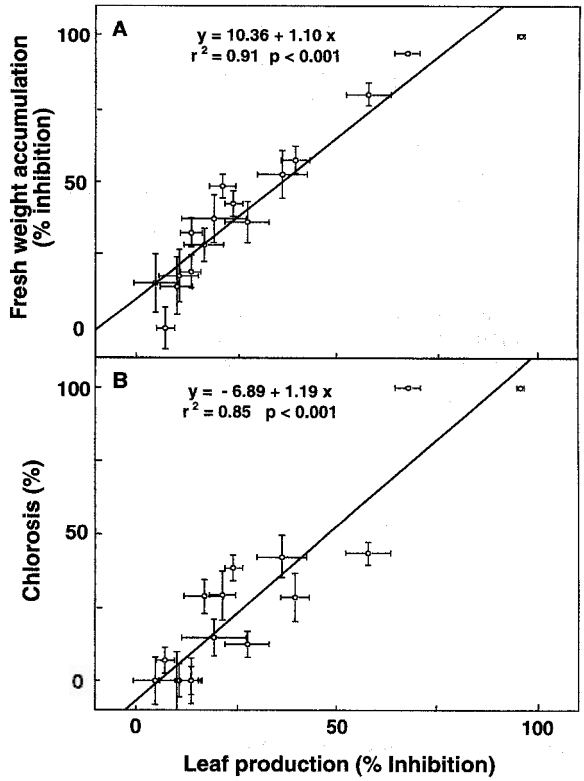


Fig. 2. Comparison of chlorosis and fresh weight accumulation with leaf production in *Lemna gibba*. Plants were grown with intact polycyclic aromatic hydrocarbons as in Figure 1. After 8 d, growth inhibition (as in Fig. 1), fresh weight, and chlorophyll content were determined, and tabulated as percent relative to the controls. Panel **A**: fresh weight accumulation versus growth inhibition. Panel **B**: chlorosis (diminished chlorophyll content) versus growth inhibition. Linear regressions were performed with SYSTAT; fit ($r^2$) and significance ($p$) are given. Error bars represent standard error of the mean ($n$ = 9) as in Figure 1.

for ANT, BAA, BBA, and BAP. Relative to the intact chemicals, the toxicity of 14 of the 16 compounds increased dramatically following photomodification; the exceptions were ANT and DAA, which showed only slight increases.

### *Comparison of leaf production, fresh weight accumulation and chlorosis as measures of toxicity*

Although the number of leaves produced in a given length of time generally serves as an excellent measure of toxicity for *L. gibba* [16,19], this approach was validated by comparing leaf production to fresh weight accumulation (another measure of growth) and chlorophyll content (a physiologic measure of stress). For the 16 PAHs tested, the two alternate measures of toxicity correlated strongly with inhibition of growth as measured by leaf count ($r^2 \geq 0.85$, $p < 0.001$) (Fig. 2). In both cases, the equations comparing the data had slopes approaching unity and intercepts close to the origin. For purposes of modeling PAH toxicity, growth inhibition based on leaf count can be concluded to be a reasonable measure of toxic impact.

### *Basis for the predictive model of toxicity*

We demonstrated [8] that the photoinduced toxicity of PAHs to *L. gibbba* can be described by the photochemical dynamics of PAHs in a two-compartment system: aqueous solution (growth medium containing intact and photomodified PAHs) and tissue (*L. gibba* leaves containing intact and photomodified PAHs). This resulted in a theoretical model, based on first principles of chemical dynamics, that related toxicity to a sum of the photosensitization activity of intact PAHs and the biological activity of photomodified PAHs. The physical constants and toxicity data in Table 1 for the predictive model were chosen based on the theoretical model [8]. As in the previous model, $C_A$ and $C_L$ are intact PAHs in the aqueous medium and leaf tissue, respectively, and $P_A$ and $P_L$ are photomodified PAHs in the aqueous medium and leaf tissue, respectively.

Photosensitization reactions initiated by PAHs proceed via excited singlet-state oxygen ($^1O_2$), the formation of which depends on the concentration of excited triplet-state PAHs in the leaf ($^3C_1$). Formation of $^3C_L$ is dependent on the concentration of the intact PAH in the leaf, $[C_L]$, the integral ($J$) of the overlap between the spectrum of the SSR source and the absorption spectrum of the PAH, and the quantum yield ($\varphi$) of excited triplet-state formation on following absorbance of a photon [20–23]. A photosensitization factor (PSF) can be described as

$$PSF = f\{[C_L], \varphi, J\} \quad (1)$$

where $[C_L]$ is the extent of uptake for each PAH in intact form (i.e., the extent of uptake in the absence of photomodification). If uptake data were unavailable, the log of the octanol/water partition coefficient $K_{ow}$ could be submitted [3]. The PSF represents the probability of *L. gibba* assimilating a given intact PAH, the probability of that PAH absorbing a photon generated by the SSR source, and the probability of PAH triplet-state formation after photonic excitation. The probability of absorbing a photon incorporates the singlet-state energy of a PAH, as the absorption spectrum summarizes the excited singlet-state energies of a PAH. The PSF does not, however, include triplet-state energy or the triplet-state lifetime, because all PAH excited triplet states have sufficient energy to excite ground-state $^3O_2$ to $^1O_2$ and the triplet-state lifetimes of PAHs

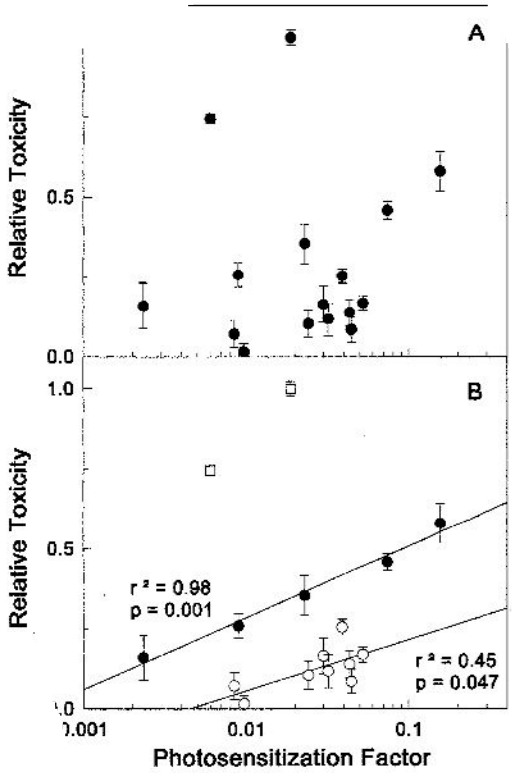


Fig. 3. Photoinduced toxicity of intact polycyclic aromatic hydrocarbons (PAHs) to *Lemna gibba* versus the photosensitization factor (PSF). Toxicity data for intact PAHs from Figure 1 (normalized from 0 to 1) were plotted against the PSF (from Table 1). When all values are included in the analysis no significant correlation to toxicity was observed (panel **A**). When two PAHs (ANT and BAA, open squares) were excluded, two independent log-linear regressions could be drawn using SYSTAT (closed circles, open circles, panel **B**). Error bars represent standard error of the mean ($n$ = 9). PAH abbreviations as in Figure 1.

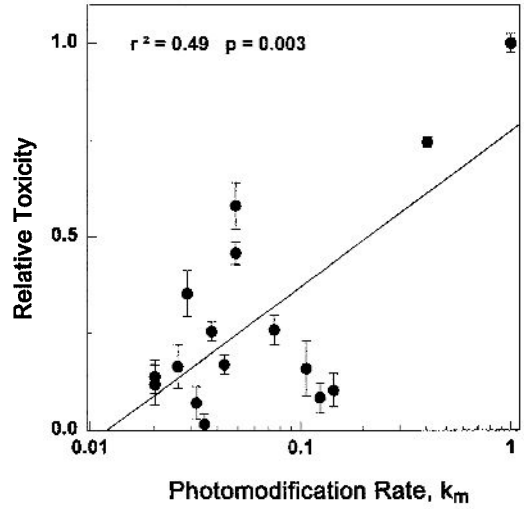


Fig. 4. Photoinduced toxicity of intact polycyclic aromatic hydrocarbons to *Lemna gibba* versus normalized rate of photomodification. The normalized toxicity data (as in Fig. 3) were plotted against the normalized rate constant for photomodification, $k_m^n$ (normalized, Table 1). Error bars represent standard error of the mean ($n$ = 9). Log-linear regression was performed with SYSTAT.

are sufficiently long that the formation of $^1O_2$ is highly efficient [8].

Photomodified PAHs are generated with pseudo-first-order kinetics [6,12]. The rate constants for photomodification, $k_m$, can be derived from the half-life ($t_{1/2}$) of each chemical in SSR using an exponential decay function [8]. The photomodified PAHs will be taken up by *L. gibba* to bioconcentrations of $[P_L]$, which react at a rate $k_d$ with plant biomolecules (G) required for growth [8]. Thus, the effects of the photomodified PAHs on *L. gibba* can be described by a photomodification factor (PMF) that is a function of $k_m$, $[P_L]$, and $k_d$

$$\text{PMF} = f\{k_m, [P_L], k_d\} \quad (2)$$

Based on the theoretical model [8] and experimental observations [17], uptake of photoproducts is much faster than the rate of photomodification of $C_A$. Furthermore, in the theoretical model [8], the PMCs were found to only vary over about one order of magnitude, implying that the photoproducts of the PAHs tested have similar uptake potential. Hence, photomodification in the aqueous medium is the rate-limiting step for generation of $P_L$ and $[P_L]$ can be excluded from the equation. In addition, $k_d$ will be proportional to the toxicity of the photomodified PAHs, $T_{pm}$. The PMF can then be expressed by

$$\text{PMF} = f\{k_m, T_{pm}\} \quad (3)$$

Because the PMF and PSF are predicted to additively contribute to toxicity, the QSAR will be proportional to the sum of the two functions for these factors:

$$\begin{aligned}\text{toxicity} &= f\{\text{PSF} + \text{PMF}\} \\ &= f\{[C_L], \varphi, J\} + f\{k_m, T_{pm}\}\end{aligned} \quad (4)$$

Although the theoretical QSAR model was based on the sum of a PSC and a PMC for each PAH [8], either the PSF or the PMF or the rate of photomodification alone possibly will be sufficient to predict toxicity. Also, that the sum of the PSF and the rate of photomodification possibly will be sufficient without the need for the full PMF. Because the PMF contains an empirical measure of toxicity ($T_{pm}$), use of only $k_m$ in our model would be desirable as this would make the model predictive rather than explanatory.

### *Relationship of toxicity to the PSF*

The PSF was calculated as a product of three independent parameters, $[C_L]$, $\varphi$, and $J$, which were normalized (normalized value = data point ÷ highest value) and multiplied together to give the PSF (Table 1). A plot of growth inhibition versus PSF on a log-linear scale (Fig. 3A) did not reveal an obvious relationship. However, if two of the PAHs (ANT and BAA) were excluded, two independent log-linear regressions were found through two distinct clusters of PAHs (Fig. 3B). Note, ANT and BAA were excluded because they are highly toxic in photomodified form and their photomodification is rapid. Also, we attribute no real meaning to the two groupings of chemicals in the regressions (Fig. 3B) other than to show that relationships between toxicity and the PSF can be observed.

### *Relationship of toxicity to the rate of PAH photomodification*

As outlined above, theoretical basis exists for the dependence of toxicity on the rate of PAH photomodification in SSR, represented as $k_m$, an exponential decay rate constant. The values of $k_m$ were normalized to unity and plotted against toxicity of the intact chemicals. A weak relationship of limited predictive capacity was apparent (Fig. 4; $r^2 = 0.49, p = 0.003$).

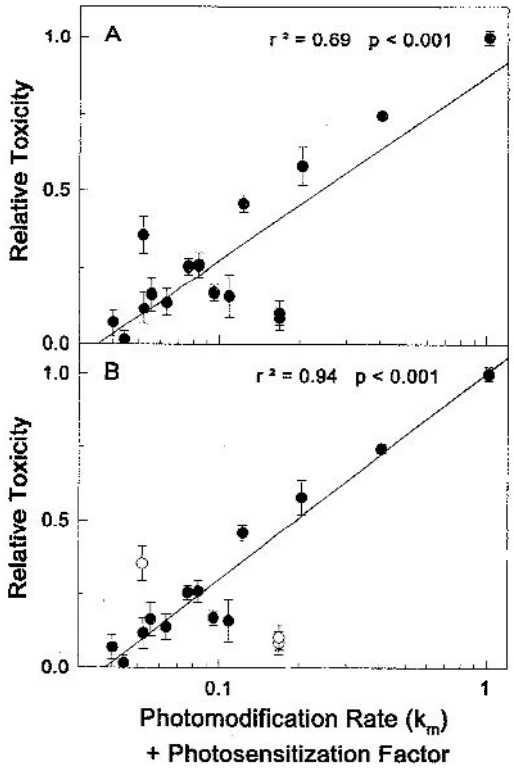


Fig. 5. Photoinduced toxicity of intact polycyclic aromatic hydrocarbons (PAHs) to *Lemna gibba* versus the sum of the photosensitization factor (PSF) and the normalized photomodification rate constant, $k_m^n$. The normalized toxicity data were used as in Figure 3. The normalized values of $k_m$ and PSFs (Table 1) were summed and plotted against the normalized growth inhibition data. The log-linear regression performed with SYSTAT in panel **A** includes all data points. The log-linear regression in panel **B** excluded three PAHs (DAA, PHE, and BBF). Error bars represent standard error of the mean ($n$ = 9). PAH abbreviations as in Figure 1.

### *Relationship of toxicity to the PSF and the rate of photomodification*

The normalized values for $k_m$ and the PSF were summed and plotted against toxicity to determine their predictive capacity. A good correlation between toxicity and the combined factors was obtained when all the PAHs were used in the regression (Fig. 5A; $r^2 = 0.69$, $p < 0.001$). Three outlying PAHs (DAA, PHE, and BBF) occurred, which, when removed from the regression analysis, dramatically improved the fit of the regression (Fig. 5B; $r^2 = 0.94$, $p < 0.001$). Hence, this model has excellent predictive capacity for 13 of the 16 PAHs investigated. For PHE and DAA, the model over-estimated toxicity, and for BBF toxicity was underestimated.

### *Relationship of toxicity to the PMF and the PSF*

Because the relationship in Figure 5 has three outliers, a factor is probably missing from the QSAR based on the sum of the $k_m$ and the PSF. Indeed, the photomodification rate does not represent a complete PMF; the relative toxicity of the photomodified PAHs should be a important factor. For a complete QSAR of photoinduced toxicity where toxicity $= f\{\text{PSF} + \text{PMF}\} = f\{[C_L], \varphi, J\} + f\{k_m, T_{pm}\}$, the operator $T_{pm}$ must be used. In this model, $T_{pm}$ is the toxicity of the photomodified PAHs and its analog in the theoretical model is the rate constant, $k_d$, for reaction of photomodified PAHs with G [8].

The PMF was generated by multiplying the normalized values of $k_m$ and $T_{pm}$ for each PAH (Table 1), and plotted against toxicity (Fig. 6). This manipulation slightly improved the correlation over using normalized $k_m$ alone (compare Figs. 4 and 6), but not enough to fully explain toxicity. Therefore, the PSF and the PMF for each PAH were summed and plotted against toxicity (Fig. 7), resulting in a relationship with a correlation of high significance ($r^2 = 0.88$; $p < 0.001$). However, the QSAR model becomes explanatory with addition of $T_{pm}$, as empirical values for toxicity of photomodified PAHs were used to generate the model.

In the above model, the PSF and PMF were treated as equal

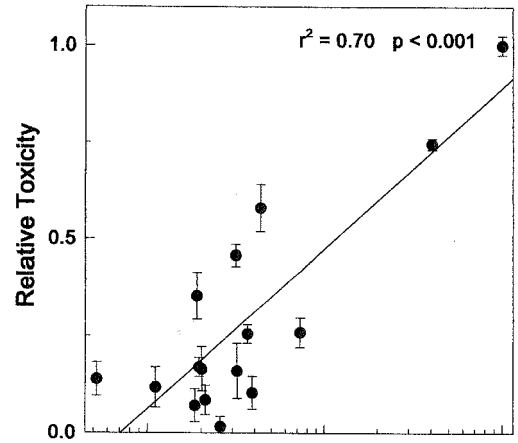


Fig. 6. Photoinduced toxicity of intact polycyclic aromatic hydrocarbons (PAHs) versus the photomodification factor (PMF). Normalized data for inhibition of growth were used as in Figure 3. The PMF was generated by multiplying the normalized values for the normalized rate constant for photomodification, $k_m$, by the normalized values for the toxicity of a photomodified PAH, $T_{pm}$. Log-linear regression analysis was performed with SYSTAT. Error bars represent standard error of the mean ($n$ = 9).

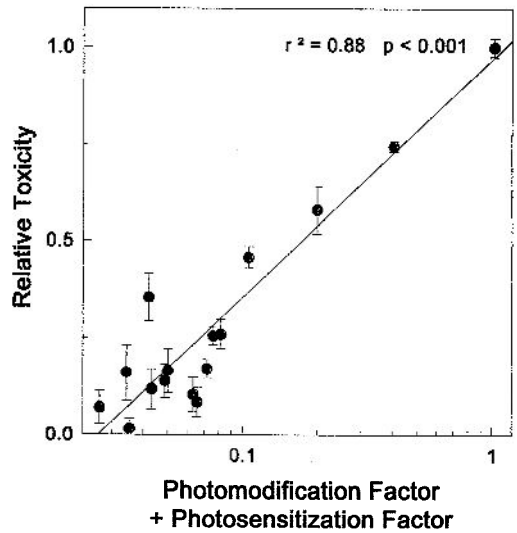


Fig. 7. Photoinduced toxicity of intact polycyclic aromatic hydrocarbons versus the sum of the photomodification factor (PMF) and photosensitization factor (PSF). Normalized toxicity data were used as in Figure 3. The PSF and the PMF (Table 1) were summed and then plotted against growth inhibition. Log-linear regression was performed with SYSTAT. Error bars represent standard error of the mean ($n$ = 9).

contributors to toxicity. However, to understand how each factor independently contributes to toxicity, multiple regression analysis was performed. A strong correlation ($r^2 = 0.85$) was obtained and described by

$$\text{toxicity} = 1.30 + 0.09 \log(\text{PSF}) + 0.20 \log(\text{PMF}) \quad (5)$$

The regression depends significantly on both the PSF ($p = 0.017$) and the PMF ($p = 0.001$). This indicates that both processes play key roles in photoinduced toxicity.

## DISCUSSION

Predictive and explanatory models for the photoinduced toxicity of PAHs were generated based on the theory described in the companion paper [8]. The attempt to formulate a purely predictive model of toxicity based solely on photophysical descriptors ($k_m$ + PSF) was modestly successful; the toxicity of 13 out of 16 PAHs was accurately predicted. The photophysical descriptors are all measurable physical properties of the chemicals that do not require toxicity testing for determination. These include the rates of photomodification and uptake of the chemicals, the triplet-state quantum yields, and the absorbance spectra. To improve the model, toxicity of the photomodified PAHs, $T_{pm}$, was added. This takes away the predictivity of the model, making it explanatory. Multiple regression analysis of the explanatory model (PSF + PMF) revealed that both photosensitization and photomodification play significant roles in toxicity. This implies that intact PAHs are active photosensitizers, until photomodified, at which point the photoproducts exert a negative biological impact along with the remaining intact PAHs.

It may be possible to find a substitute for $T_{pm}$ in the PMF and make the full model predictive, that is, use a factor describing the constant $k_d$ as presented in the theoretical model [8]. $T_{pm}$ might be replaced by determining which species in the mixture of photomodification products contribute the most to toxicity. Alternatively, the general reactivity of the mixtures of the photomodified chemicals with isolated membranes or the uptake potential of the mixtures might be used in place of toxicity of the photomodified PAHs. Finally, we are currently developing computer modeling techniques describing reactivity based on chemical structure and this might provide relative values for $k_d$ [24].

Many studies on photoinduced PAH toxicity have only examined effects of the intact PAHs. These studies have shown that photosensitization reactions are an important aspect of photoactivity [3,25–27]. Although a significant relationship between toxicity and the PSF for the 16 PAHs tested was not evident (Fig. 3), when ANT and BAA were excluded from the regression, two independent regressions were observed for the 14 remaining PAHs. This suggests that photosensitization plays a major role in toxicity, but alone it is not predictive of toxic strength. Importantly, the high phototoxicity of ANT and BAA cannot be addressed by photosensitization. The photomodification products of ANT and BAA are highly toxic (Fig. 1), and ANT and BAA are photomodified rapidly in SSR ($t_{1/2}$ = 2 and 5 h, respectively). Reflecting this, both the theoretical and explanatory models gave ANT and BAA the highest PMCs and PMFs, as well as low PSCs and PSFs.

The results of our recent studies [6,13,28] and the work reported here show that photomodified PAHs are biologically active. Interestingly, the order of toxic strength for intact PAHs exhibited a weak correlation to their rates of photomodification (Fig. 4). For All 16 PAHs tested, the mixtures of photoproducts derived from extensive photomodification of a given PAH were more toxic than the intact PAHs in SSR. This is reminiscent of the increase in PAH toxicity and mutagenicity resulting from cytochrome P450-mediated oxidation in animals [29–31].

Even though the photomodification rates only correlated weakly with toxicity, comparison of photoinduced toxicity with the photomodification rate for a few specific PAHs is worthwhile. The photomodification rate of FLA is about the same as that of BAP ($t_{1/2}$ = 40 and 52 h, respectively), whereas the toxicity of intact FLA is greater than that of intact BAP (50 and 20% growth inhibition, respectively). In this case, the similar rates of photomodification cannot fully explain the greater toxicity of FLA, especially because photomodified FLA and photomodified BAP have similar toxicities. Comparing FLA with PHE, we find that photomodification of FLA is slower than that of PHE ($t_{1/2}$ = 40 and 14 h, respectively), whereas the toxicity of intact FLA is significantly greater than the toxicity of intact PHE (50 and 15%, respectively). Again, the rate of photomodification alone cannot fully explain photoinduced toxicity. Fluoranthene has been regarded as an excellent example of a PAH that exerts toxicity via photosensitized production of $^1O_2$ [3,25,32]. Fluoranthene has a higher quantum yield for triplet-state formation than either BAP or PHE (Table 1), which means FLA has a greater probability of generating $^1O_2$ via a type II photosensitization reaction [1,8]. This fact is reflected in both the theoretical and explanatory models where FLA had the highest PSC [8] and PSF (Table 1).

An indication of the importance of both the PSF and PMF in toxicity is the relative strength of the two factors. In both this model and the theoretical model [8] about half the PAHs have a PSF (or PSC) greater than the PMF (or PMC). Additionally, for 10 of the 16 PAHs the same factor dominates in both the theoretical and explanatory models. Although obviously not a perfect fit, both models show similar trends. Importantly, they both demonstrate that photosensitization and photomodification must be combined additively to explain photoinduced toxicity of PAHs.

The discrepancies of the theoretical [8] and explanatory models might be explained by a number of factors. First, each empirical measurement made (toxicity, uptake, and photomodification rate) has at least a 5 to 10% experimental error. Additionally, for each PAH 20 to 30 photoproducts can be generated [13], the toxicity of which will vary depending on the mixture of photoproducts present at any moment during a toxicity test. For some PAHs the photoproducts are highly toxic (ANT and BAA), for others the photoproducts have relatively low impacts (BGP and DAA). Moreover, as discussed in the companion paper [8], due to PAH uptake, the rates of photomodification could be different in the presence of plant tissue than as measured in aqueous medium without plants. Secondly, the data for the triple-state quantum yield of PAHs, which came from the literature, were collected under low temperature (77 K) in organic solvents [20–23]. Finally, other unidentified parameters contributing to toxicity could exist that were not used in our modeling.

Based on this modeling work, an important consideration is the effects of photomodified PAHs on target organisms other than plants. Recently, we found that phenanthrenquinone, the primary photoproduct of PHE, is toxic to *Photobacterium phosphurium* [13] and to *Daphna magna* (unpublished observations). However, the *L. gibba* model presented here may not extend to animals and bacteria; they have different met-

abolic systems and likely the mechanisms of toxicity of photomodified PAHs will be different. Importantly, in animal toxicity testing the chemical to tissue ratio is usually lower than with plants. This is because depletion of chemicals from the medium by plant uptake becomes a significant factor in the toxicity assay. Thus, the concentrations of PAHs used in this study are higher than those used in analogous animal studies [3,6,25,26,32] and this QSAR model might require modification before application to animal systems.

Because the interactions of environmental contaminants with biological organisms are very complicated, attempts at modeling relationships between chemical structure and toxicity without considering internal and external factors will fail to fully explain the impacts. Understanding the reaction mechanisms is key to predicting toxicity of contaminants in the environment. These mechanisms are the basis for elucidating which interactions between a given chemical and the environmental surroundings have the greatest impact on the hazards of the chemical. These interactions include modification of the contaminant in the environment. If these relationships between the chemical and the environment are understood, toxicity of contaminants in the environment can, to a greater degree, be predicted based on the chemical and biological properties of these reactions. It is clear from the research presented here that describing the interactions of modifying factors in the environment, such as sunlight, is one of the keys for modeling toxicity and evaluating the risks of environmental contaminants.

*Acknowledgement*—We acknowledge W. Taylor, N. Bols, P. Mezey, and members of the Greenberg and Dixon labs for fruitful discussions. We thank L.F. Zeiler for her time and effort helping the authors develop and edit this manuscript. This research was supported by grants from the Canadian Network of Toxicology Centers and the National Science and Engineering Research Council to B.M. Greenberg and D.G. Dixon.

## REFERENCES

1. **Hermens, J.L.M.** 1989. Quantitative structure activity relationships of environmental pollutants. In O. Hutzinger ed., *Handbook of Environmental Chemistry,* Vol. II E—Reactions and Processes Springer-Verlag, Berlin, Germany, pp. 111–162.
2. **Hermens, J.L.M.** and **A. Opperhuizen,** eds. 1991. *QSAR in Environmental Toxicology—IV.* Elsevier, Amsterdam, The Netherlands.
3. **Newsted, J.L.** and **J.P. Giesy.** 1987. Predictive models for photoinduced acute toxicity of polycyclic aromatic hydrocarbons to *Daphna magna,* Strauss (Cladocera, Crustacea). *Environ. Toxicol. Chem.* **6**:445–461.
4. **Cooper, W.J.** and **F.L. Herr.** 1987. Introduction and overview. In R.G. Zika and W.J. Cooper, eds., *Photochemistry of Environmental Aquatic Systems.* ACS Symposium Series 327. American Chemical Society, Washington, DC, pp. 1–8.
5. **Larson, R.A.** and **M.R. Berenbaum.** 1988. Environmental phototoxicity. *Environ. Sci. Technol.* **22**:354–360.
6. **Huang, X.-D., D.G. Dixon** and **B.M. Greenberg.** 1993. Impacts of ultraviolet radiation and photomodification on the toxicity of polycyclic aromatic hydrocarbons to the higher plant *Lemna gibba* L. G-3 (duckweed). *Environ. Toxicol. Chem.* **12**:1067–1077.
7. **Foote, C.S.** 1991. Definition of type I and type II photosensitized oxidation. *Photochem. Photobiol.* **54**:659.
8. **Krylov, S.N., X.-D. Huang, L.F. Zeiler, D.G. Dixon** and **B.M. Greenberg.** 1997. Mechanistic quantitative structure–activity relationship model for the photoinduced toxicity of polycyclic aromatic hydrocarbons: I. Physical model based on chemical kinetics in a two-compartment system. *Environ. Toxicol. Chem.* **16**: 2283–2295.
9. **Foote, C.S.** 1987. Type I and type II mechanisms in photodynamic action. In J.R. Heitz and K.R. Downum, eds., *Light-Activated Pesticides.* ACS Symposium Series 339 American Chemical Society, Washington, DC pp. 22–38.
10. **Packer, L.,** ed. 1984. *Oxygen Radicals in Biological Systems.* Vol. 105. Academic Press, San Diego, CA, USA.
11. **Halliwell, B.** and **J.M.C. Gutteridge.** 1985. *Free Radicals in Biology and Medicine.* Clarendon, Oxford, UK.
12. **Katz, M., C. Chan, H. Tosine** and **T. Sakuma.** 1979. Relative rates of photochemical and biological oxidation (in vitro) of polynuclear aromatic hydrocarbons. In P.W. Jones and P. Leber, eds., *Polynuclear Aromatic Hydrocarbons.* Ann Arbor Science, Ann Arbor, MI, USA, pp. 171–189.
13. **McConkey, B.J., C.L. Duxbury, D.G. Dixon** and **B.M. Greenberg.** 1997. Toxicity of a PAH photooxidation product to the bacteria *Photobacterium phosphoreum* and the duckweed *Lemna gibba*: Effects of phenanthrene and its primary photoproduct, phenanthrenequinone. *Environ. Toxicol. Chem.* **16**:892–899.
14. **Ren, L., X.-D. Huang, B.J. McConkey, D.G. Dixon** and **B.M. Greenberg.** 1994. Photoinduced toxicity of three polycyclic aromatic hydrocarbons (fluoranthene, pyrene, and naphthalene) to the duckweed *Lemna gibba* L. G-3. *Ecotoxicol. Environ. Saf.* **28**: 160–171.
15. **American Society for Testing and Materials.** 1995. Standard guide for using lighting in laboratory testing. E 1733-95. In *Annual Book of ASTM Standards,* Volume 11.05. Philadelphia, PA, p. 11.
16. **Greenberg, B.M., X.-D. Huang** and **D.G. Dixon.** 1992. Applications of the aquatic higher-plant *Lemna gibba* for ecotoxicological assessment. *J. Aquat. Ecosyst. Health* **1**:147–155.
17. **Duxbury, C.L., D.G. Dixon** and **B.M. Greenberg.** 1997. Effects of simulated solar radiation on the bioaccumulation of polycyclic aromatic hydrocarbons by the duckweed *Lemna gibba. Environ. Toxicol. Chem.* **16**:1739–1748.
18. **tenHulscher, T.E.M., L.E. vanderVelde** and **W.A. Bruggeman.** 1992. Temperature dependence of Henry's law constants for selected chlorobenzenes, polychlorinated biphenyls and polycylic aromatic hydrocarbons. *Environ. Toxicol. Chem.* **11**:1595–1603.
19. **Wang, W.C.** 1991. Literature review on higher plants for toxicity testing. *Water Air Soil Pollut.* **59**:381–400.
20. **Lakowicz, J.R.** 1983. *Principles of Fluorescence Spectroscopy.* Plenum, New York, NY, USA.
21. **Commission of the European Communities.** 1985. *Spectral Atlas of Polycylic Aromatic Compounds.* D. Reidel, Dordrecht, The Netherlands.
22. **Nakhimovsky, L.** 1989. *Handbook of Low Temperature Electronic Spectra of Polycyclic Aromatic Hydrocarbons.* Elsevier, Amsterdam, The Netherlands.
23. **Lakowicz, J.R.** 1991. *Topics in Fluorescence Spectroscopy,* Vol. 1–2. Plenum, New York, NY, USA.
24. **Mezey, P.G., Z. Zimpel, P. Warburton, P.D. Walker, D.G. Irvine, D.G. Dixon** and **B.G. Greenberg.** 1996. A high-resolution shape-fragment MEDLA database for toxicological shape analysis of PAHs. *J. Chem. Inf. Comput. Sci.* **36**:602–611.
25. **Morgan, D.D., D. Warshawsky** and **T. Atkinson.** 1977. The relationship between carcinogenic activities of polycyclic aromatic hydrocarbons and their singlet, triplet, and singlet–triplet splitting energies and phosphorescence lifetimes. *Photochem. Photobiol.* **25**:31–38.
26. **Schoeny, R., T. Cody, D. Warshawsky** and **M. Radike.** 1988. Metabolism of mutagenic polycyclic aromatic hydrocarbons by photosynthetic algal species. *Mutat. Res.* **197**:289–302.
27. **Greenberg, B.M., X.-D. Huang, D.G. Dixon, L. Ren, B.J. McConkey** and **C.L. Duxbury.** 1993. Quantitative structure activity relationships for the photoinduced toxicity of polycyclic aromatic hydrocarbons to plants—A preliminary model. In J.W. Gorsuch, F.J. Dwyer, C.G. Ingersoll and T.W. La Point, eds., *Environmental Toxicology and Risk Assessment,* Vol. 2. STP 1216. American Society for Testing and Materials, Philadelphia, PA, pp. 369–378.
28. **Ren, L., L.F. Zeiler, D.G. Dixon** and **B.M. Greenberg.** 1996. Photoinduced effects of polycyclic aromatic hydrocarbons on *Brassica napus* (canola) during germination and early seedling development. *Ecotoxicol. Environ. Saf.* **33**:73–80.
29. **Yang, S.K., D.W. McCourt, P.P. Roller** and **H.V. Gelboin.** 1976. Enzymatic conversion of benzo(*a*)pyrene leading predominantly to the diol-epoxide *r*-7,*t*-8-dihydroxy-*t*-9,10-oxy-7,8,9,10-tetrahydroxybenzo(*a*)pyrene through a single enantiomer of *r*-7,*t*-

8-dihydroxy-7, 8-dihyrobenzo(*a*)pyrene. *Proc. Natl. Acad. Sci.* USA **73**:2594–2598.

30. **Shimada, T.** and **S.-I. Nakamura.** 1987. Cytochrome P-450 mediated activation of procarcinogens and promutagens to DNA damaging products by measuring expression of umu gene in *Salmonella typhimurium* TA 1535/pSK1002. *Biochem. Pharmacol.* **36**:1979–1987.
31. **Harvey, R.G., C. Cortez, T. Sugiyama, Y. Ito, T.W. Sawyer** and **J. DiGiovanni.** 1988. Biologically active dihydrodiol metabolites of polycyclic aromatic hydrocarbons structurally related to the potent carcinogenic hydrocarbon 7,12-dimethylbenz(*a*)anthracene. *J. Med. Chem.* **31**:154–159.
32. **Mekenyan, O.G., G.T. Ankley, G.D. Veith** and **D.J. Call.** 1994. QSAR for photoinduced toxicity: I. Acute lethality of polycyclic aromatic hydrocarbons to *Daphnia magna*. *Chemosphere* **28**: 567–582.